Tropical cyclones shift poleward more over Land than over Ocean

Authors: B. Zhang[1*,2], J. X. L. Wang[3], M. C. Wheeler[4], Y. Feng[2], Q. Wan[2]

Affiliations:

[1]NOAA NCEP Environmental Modeling Center, College Park, MD 20740, USA.

[2] China Meteorological Administration/ Guangdong Provincial Key Laboratory of Regional Numerical Weather Prediction, China Meteorological Administration, Guangzhou, China

[3]NOAA/Air Resources Laboratory, College Park, MD 20740, USA.

[4]Bureau of Meteorology, Melbourne, Victoria, Australia.

Corresponding author. E-mail: banglin.zhang@noaa.gov

Abstract: The latitudes of all Northern Hemisphere tropical cyclones (TCs) from the National Hurricane Center (NHC)/Joint Typhoon Warning Center (JTWC) best track data are used to investigate their poleward migration from 1970 to 2017. The annual means of the track latitudes are calculated for tropical storms, hurricanes/typhoons, and all storms over land and ocean, respectively. The analysis of the annual time series shows that TCs have shifted poleward more over land than over ocean, particularly for strong hurricanes and typhoons. For TC landfall, the analysis show hurricanes and typhoons made landfall gradually towards higher latitudes from 1970 to the early 2000s, and then the poleward trend levels off. The complexities of the poleward shifts are further compounded by the fact that the shifts are non-uniform from basin to basin. The predominant trend in the North Atlantic is the equatorward shift over ocean, while over the western Pacific it is a poleward shift over land. Poleward shifts of tropical cyclone positions may be attributable to the land-ocean contrast of surface temperature warming trends.

One Sentence Summary: Tropical cyclones shift poleward more over land than over ocean, particularly for strong hurricanes and typhoons

Main Text:

Long term changes in tropical cyclone (TC) activity are one of the more important aspects of climate change, and have gained considerable attention in the climate community (1-4). One of the earliest studies was by P.J. Webster et al., who found that although the number of TCs and TC days had decreased in all basins except the North Atlantic in the decade since 1995, there was a great increase in the number and proportion of very strong cyclones (5). Since then, more studies were conducted with other TC datasets for trends in TC activity, such as TC frequency, intensity, longevity, and the potential destructive index (PDI) in regional basins or the whole globe (6-10). Numerical simulations mostly indicate fewer tropical cyclones globally in a warmer climate, but an increase in average cyclone intensity, precipitation rates, and the number and occurrence days of very intense category 4 and 5 storms (11-14).

The long-term change of TC geographic distribution and the long-term shift of TC tracks is another important aspect. It is of importance to know if climate change is causing TCs to be experienced in parts of the world now free from them or to cease in regions they now trouble (15). For long term shifts of TC geographic distribution, studies have shown that the annual mean latitude of TC lifetime maximum intensity (LMI) is shifting toward the poles, with more storms reaching their maximum strength at higher latitudes (16). Further, the mean longitude of TCs that first reached an intensity of 25 knots shows a westward shift for western North Pacific TCs (17). The LMI reduced some uncertainties of individual cyclone intensity estimations in best track data sets, and has been used to investigate the TC intensity and frequency trend, the rapid intensification and the bimodal distribution of TC intensity (18-20), and the poleward shifts of the latitudes where TCs approach their LMI (21-23).

However, as the LMI parameter uses only one latitudinal value for each TC, the rich information of TC position as recorded in the best track data is under-utilized. For example, we have the best track data for Hurricane Sandy in 2012 listed in Table S1 of the Supplementary Information (SI) section and Hurricane Lisa in 2010 listed in Table S2. The LMI latitudes for Hurricanes Sandy and Lisa are 20.05^{o}N and 20.4^{o}N, respectively, which are only 0.35 degree apart. Hurricane Sandy reached its LMI latitude far to the south of the most impacted area in northeastern USA, and was a land-falling storm. But Hurricane Lisa weakened quickly after reaching its maximum intensity over ocean. These very close LMI latitudes hide the very different patterns illustrated by Sandy and Lisa. Moreover, the landings of most TCs occur after their maximum intensity. Therefore, it would be almost impossible to use the LMI parameter to investigate the climate shift of TCs over land.

To utilize as much as possible the information provided by the TC best track data, we use the full track latitudes to calculate their annual means. The computations are done separately for two sub-categories of TCs: tropical storms (TS) with maximum wind (Vmax) from 34 to 64knots, and hurricanes in the North Atlantic (NATL) basin and Eastern Pacific (EPAC) basin and typhoons in Western Pacific (WPAC) basin with Vmax greater than 64knots, all denoted as HT. Combining the groups of TS and HT is labeled as ALL (24). To further investigate the impacts of land and ocean, the computations are also discriminated for these sub-categories using the MOD44W MODIS Water Mask as the standard land/sea mask provided by Carroll et al. (25).

The 1970-2017 best-track datasets, 1970-2017 sea surface temperature data (SST), and 1979-2016 skin temperature data (SKT), were used for this study. The annual mean values for SKT and SST are calculated with June to October monthly means for each year. The SKT annual mean time series are calculated over land and ocean, respectively, spanning latitudes from Equator to 35^{o}N. In addition, the first and the last 10-year averages of SKT and SST are calculated to identify meridional and zonal shifts of surface temperature over land versus ocean under the influence of global warming. These shifts might be a contributing factor for the corresponding shifts of TC activity. The linear and quadratic curves are fit to the time series, and a P-value test is used to check if the computed trends are statistically significant (26).

The annual mean latitudes of TC track positions from 1970 to 2017 calculated from the best track data are shown in Fig. 1 for the NATL, EPAC and WPAC collectively, which covers the entire Northern Hemisphere except the North Indian Ocean. The statistics over land (upper panel) and over ocean (bottom panel) exhibit striking differences for the poleward trends.

Especially for the HT sub-category of hurricanes/typhoons, there is a pronounced poleward shift trend over land of 0.87^o of latitudes per decade, which is statistically significant. However, the same trend over ocean is only 0.19^o per decade. For TS sub-category and ALL cyclones, the poleward trends are also much larger over land than over ocean.

The intensities of hurricane/typhoon usually decrease at landfall or soon after. The obvious poleward shifts of HT over land may be indicative that the landfalls of strong storms migrate away from the Tropics, and toward higher latitudes in the Northern Hemisphere. Shown in the bottom panel of Fig. 2 are landfall latitudes from the total of 855 individual land-falling storms between the period of 1970 and 2017. Also shown in the upper panel of Fig. 2 is the annual mean landfall latitudes and the corresponding linear and quadratic trends. There is an obvious poleward shift trend, particularly from 1970 to the beginning of the current century, and it is equally interesting to note the levelling off in the poleward shift of the annual mean landfall latitude of the HT sub-category in the Northern Hemisphere since the early 2000s.

TC's usually reach their maximum intensity (i.e. LMI) over ocean, and the trends of their latitudinal locations are indicative of the TC migration more over ocean than over land. Shown in the bottom panel of Fig. 3 are the latitudes from the total of 2992 individual storms between the period of 1970 and 2017. Also shown in the upper panel of Fig. 3 is the annual mean of those LMI latitudes and the corresponding linear and quadratic trends. It is quite a surprise that the trend is negative with equatorward migration although the trend is not statistically significant. The poleward migration of 16.04 kilometers per decade with 48year best track data from 1970-2017 is quite different from the analysis by Kossin et al. (16) with 31year data from 1982 to 2012. To see the impact of time series length to trend analysis, the LMI trends have also been estimated for 1982 to 2012 (upper panel of Fig. S1 in SI) and 1982 to 2017 (bottom panel of Fig. S1 in SI), respectively, where the poleward shifts are 86.63 (consistent with Kossin et al.), and 52,86 kilometers per decade. The big trend swings come from using/not using the 1970s data during that period LMI positions had much higher latitudes.

The observations shown in Figs. 1, 2 & 3 may be partly explained by the contrasting global warming trends over land versus ocean, as shown in Fig. 4 for 1979-2016 annual mean time series of ERA-Interim (ERAi) SKT anomalies over land (upper) and oceans (bottom) from the Equator to 35^{o}N. The land-ocean contrast of surface temperature changes is a well-known phenomenon whereby large parts of the land surface undergo greater warming in response to global warming than the ocean (27-29).

Despite large and statistically significant contrasting trends in the annual-mean latitudes of TC positions over Northern Hemisphere land versus ocean, as well as the landfall latitudes of hurricanes and typhoons, substantial inter-basin changes and interannual variabilities are evident. For the NATL basin, there are small poleward shifts, which are statistically insignificant over land, as show in the upper panel of Fig. S2. However, there were very significant equatorward shifts over ocean (bottom panel of Fig. S2), opposite to the shifts for the three basins combined.

The contrasting meridional shifts of the NATL may be attributable to the different expansion directions of warm SKT over Eastern USA versus SST over the Atlantic Ocean as shown in Fig. S5 and S6. The area of SST greater than 28^{0}C expanded eastward and equatorward from the 1970s to 2010s over the Atlantic Ocean, whereas the SKT area of greater than 24^{0}C in Eastern USA expanded slightly poleward. For the WPAC basin, there is a pronounced poleward TC shift trend over land, while TC position shift is not as big over the ocean (Fig. S3). Its corresponding SKT and SST distributions are shown in Fig. S7 and S8. For the EPAC basin, land-falling TC position shift and its discussion may be trivial due to limited data sample as well as land mass. However, Fig. S4 shows overall the equatorward TC shift over ocean, which matches well with SST warm area expansion direction near coastal Mexico in Fig. S8.

With 48years of best track data, TC activity is found to shift poleward more over land than over ocean, particularly for strong hurricanes and typhoons. The averaged latitude of land-falling hurricanes and typhoons moves gradually towards higher latitudes from 1970 to early 2000s, but then the migration levels off. Meridional shifts of TC tracks are non-uniform from basin to basin. This is quite different from the migration of the LMI, which is a good indicator of TC activity over ocean. The predominant trend over the North Atlantic is the equatorward shift over ocean, while the significant trend in the western Pacific is the poleward shift over land. The contrasting poleward shifts of TC tracks over land versus ocean, as well as large inter-basin variabilities, show the complexities of poleward migrations of TC activity. Poleward shifts of TC position may be attributable to the land-ocean contrast of surface temperature warming trends and the changing areas of relative high SST over ocean versus SKT over land.

References and Notes:

1. L. Bengtsson, M. Botzet, M. Esch, *Tellus* **48A** (1996).
2. K. A. Emanuel, *Nature* **436** (2005).
3. T. R. Knutson et al., *Nature Geoscience*, **3**, doi:10.1038/ngeo779 (2010).
4. K. J.E. Walsh, *WIREs Clim Change*, doi: 10.1002/wcc.371 (2016).
5. P. J. Webster, G. J. Holland, J. A. Curry, and H.-R. Chang. *Science*, **309**, doi:10.1126/science.1116448 (2005).
6. P. J. Klotzbach, *Geophys. Res. Lett.*, **33**, L10805, doi:https://doi.org/10.1029/2006GL025881 (2006).
7. C. W. Landsea, B. A. Harper, K. Hoarau, and J. A. Knaff, *Science*, **313**, doi:https://doi.org/10.1126/science.1128448 (2006).
8. M. -C. Wu, K.-H. Yeung, W.-L. Chang, Eos, *Trans. Amer. Geophys. Union*, **87**, doi:https://doi.org/10.1029/2006EO480001 (2006).
9. Y. Kuleshov et al., *J. Geophys. Res.*, **115**, D01101, doi:https://doi.org/10.1029/2009JD012372 (2010).
10. J. P. Kossin, T. L. Olander, and K. R. Knapp, *J. Climate*, **26**, doi:https://doi.org/10.1175/JCLI-D-13-00262.1 (2013).
11. K. A. Emanuel, R. Sundararajan, J. Williams, *Bull. Amer. Meteor. Soc.*, **89** (2008).

12. T. R. Knutson et al., *J. Climate*, **26**, doi:https://doi.org/10.1175/JCLI-D-12-00539.1 (2013).
13. S. J. Camargo, *J. Climate*, **26**, doi:https://doi.org/10.1175/JCLI-D-12-00549.1 (2013).
14. T. R. Knutson et al., *J. Climate*, **28**, https://doi.org/10.1175/JCLI-D-15-0129.1 (2015).
15. J. P. Kossin, K. A. Emanuel, G. A. Vecchi, *Nature*, **509** (2014).
16. K. A. Emanuel, https://emanuel.mit.edu/anthropogenic-effects-tropical-cyclone-activity (2006).
17. L. Wu, C. Wang, B. Wang, *Geophys. Res. Lett.*, **42**, doi: 10.1002/2015GL063450 (2015).
18. J. P. Kossin, T. L. Olander, K. R. Knapp, *J. Climate*, **26** (2013).
19. D. -S. R. Park, C. -H. Ho, J. -H. Kim, *Res. Lett.*, **9**, 014008 (2014).
20. C. -Y. Lee, M. K. Tippett, A. H. Sobel, S. J. Camargo, *Nature Communications*, **7**, doi:10.1038/ncomms10625 (2016).
21. I. -J. Moon, S. -H. Kim, P. Klotzbach, J. C. Chan, *Res. Lett.*, **10** 10400 (2015).
22. R. Zhan, Y. Wang, *J. Climate*, **30** (2017).
23. S. A. Tennill, K. N. Ellis, *Atmosphere*, **8**(10) (2017).
24. B. Zhang et al., Bull. Amer. Meteor. Soc. (under review).
25. M. L. Carroll et al., *International Journal of Digital Earth*, **2** (2009).
26. J. H. McDonald, *Handbook of Biological Statistics* (Sparky House Publishing, Baltimore, Maryland, ed. 3, 2014).
27. S. Manabe, R. J. Stouffer, M. J. Spelman, K. Bryan, *J. Climate*, **4** (1991).
28. R. T. Sutton, B. -W. Dong, J. M. Gregory, *Geophys Res Lett*, **34** L02701. doi:10.1029/2006GL028164 (2007).
29. M. M. Joshi, F. H. Lambert, M. J. Webb, *Clim Dyn*, **41** (2013).
30. T. M. Smith, R. W. Reynolds, T. C. Peterson, J. Lawrimore, J Clim **21** (2008).
31. D. P. Dee et al., *Q. J. R. Meteorol. Soc.*, **137** doi:10.1002/qj.828 (2011).
32. The 1979-2017 SST data came from NOAA_ERSST_V3b data set provided by NOAA/OAR/ESRL PSD, Boulder, Colorado, USA, from their website at http://www.esrl.noaa.gov/psd/ (30). The 1970-2017 skin temperature (SKT) were monthly data from Medium-range Weather Forecasts (ECMWF) Interim re-analysis (ERAi, 31). The best-track datasets were taken from the National Hurricane Center (NHC) for the NATL and EPAC and from the Joint Typhoon Warning Center (JTWC) for the WPAC. The 1970-2017 best track data for the NATL, EPAC, and WPAC basins were downloaded from NOAA/NHC at http://ftp.nhc.noaa.gov/atcf/ and the US Navy/JTWC at http://www.usno.navy.mil/NOOC/nmfc-ph/RSS/jtwc/best_tracks/wpindex.php. We thank Prof. Emanuel of MIT, who read the draft and provided comments that greatly improved the manuscript, and the HWRF team of NOAA/NCEP/EMC for making this study possible. This study was supported by US NOAA HFIP Project.

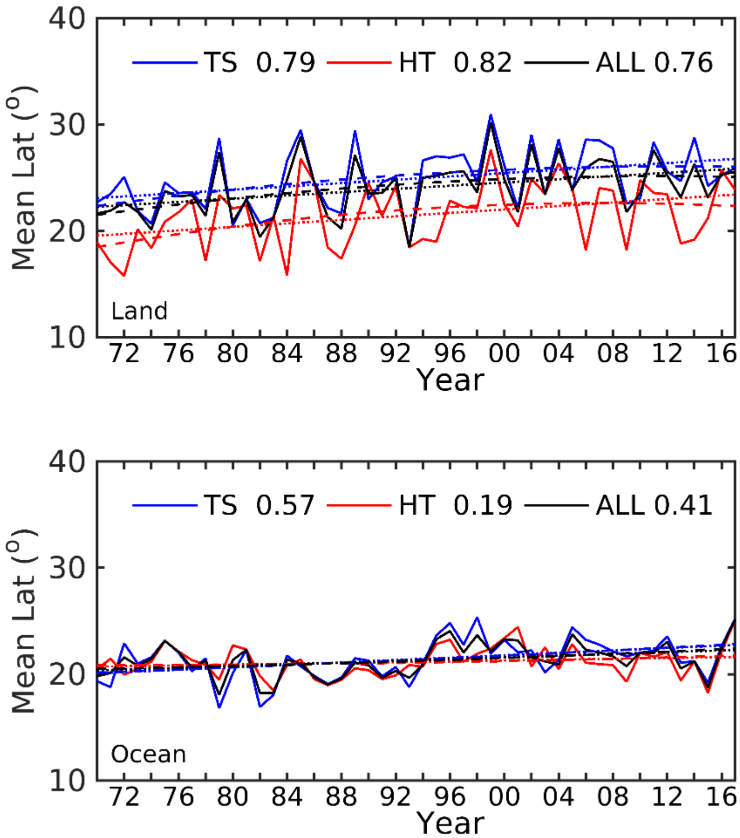

Fig. 1. 1970-2017 annual mean time series of TC latitudinal positions and their trends over land (upper) and ocean (bottom) for 3 basins combined. The blue, red, and dark solid curves are for TS, HT, and ALL storms, respectively. Dotted and dashed lines respectively show the best fit linear and quadratic trends. The linear trend values are shown in the top of each panel with unit degree per decade. All these trends are statistically significant at the 95% level.

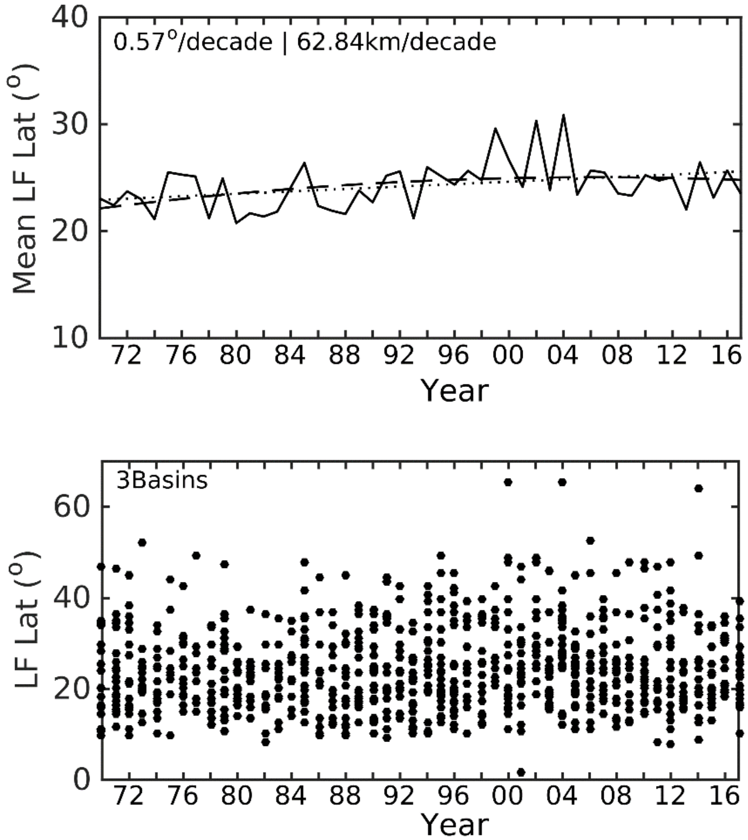

Fig. 2. 1970-2017 annual mean time series of TC landfall latitudinal positions and their trends (upper), and the individual latitudinal positions of landfall for TCs (lower), for 3 basins combined. Dotted and dashed lines respectively show the best fit linear and quadratic trends. The linear trend is 0.57° per decade, which is statistically significant at the 95% level.

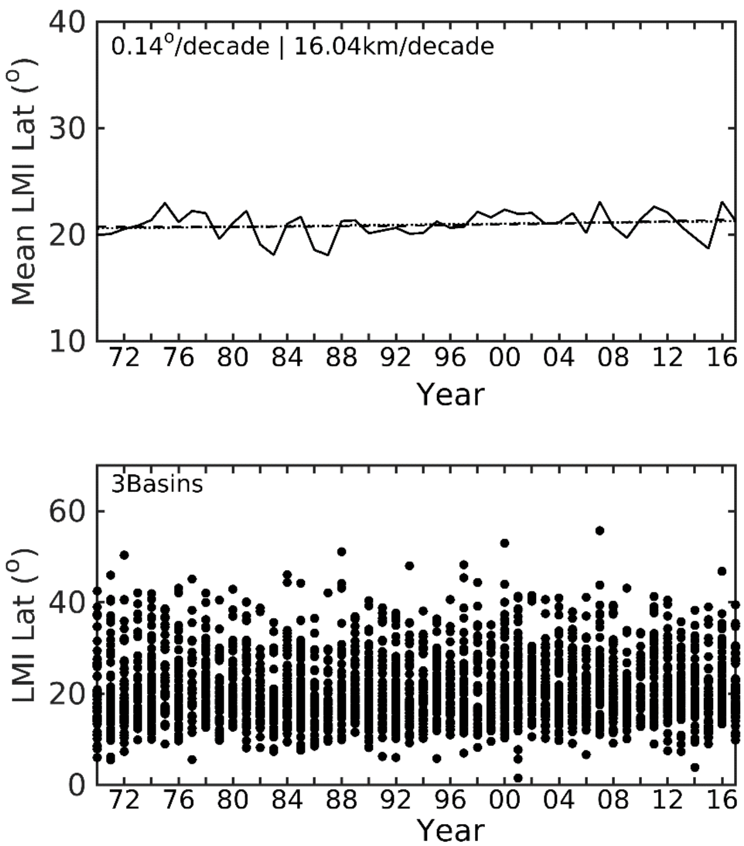

Fig. 3. As in Fig. 2, but for the TC LMI latitudes. The linear trend is only 0.10° per decade, which is not statistically significant.

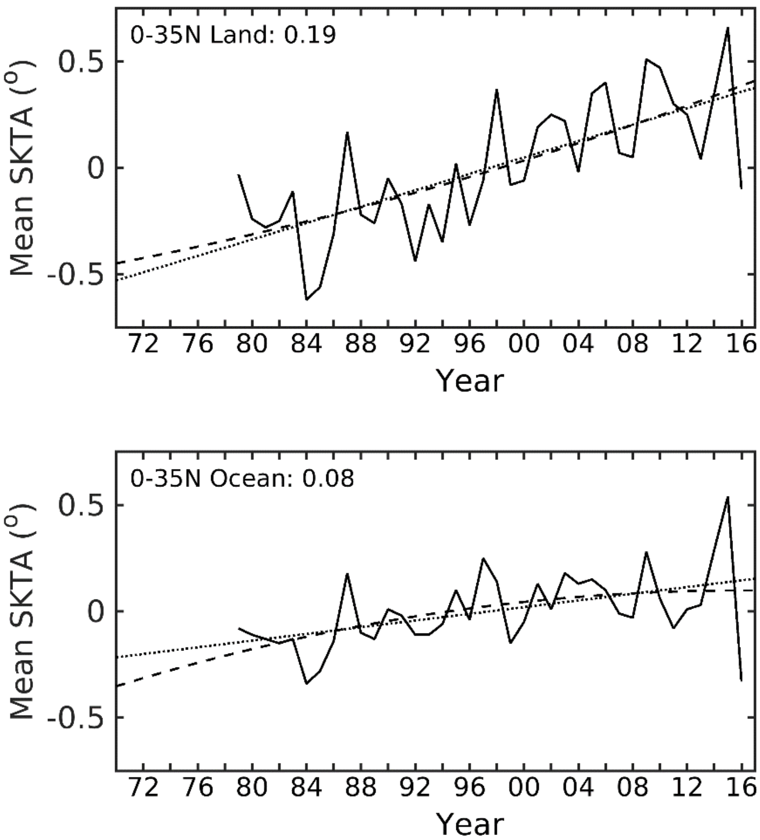

Fig. 4. 1979-2016 annual mean time series of (ERAi) SKTA over land (upper) and oceans (bottom) from the Equator to 35°N. The solid curve is for SKTA time series. Dotted and dashed lines respectively show the best fit linear and quadratic trends. The linear trend values are shown in the top of each panel with unit °C per decade, which are all statistically significant over 95%.

Supplementary Information:

Table S1. Hurricane Sandy 18L 2012 best track data, where bold red is for wind speed at its maximum, and bold blue is for speeds greater than 64 knots. The latitude of LMI for Hurricane Sandy is 20.05°N, which was far to the south of the most impacted area in the northeastern USA.

	Lat(°N)	Lon (°W)	Vmax(kts)	Date(yymmddhh)	Lat(°N)	Lon (°W)	Vmax(kts)
12102218	12.7	78.7	35	12102700	27.5	77.1	60
12102300	12.6	78.4	40	12102706	28.1	76.9	60
12102306	12.9	78.1	40	**12102712**	**28.8**	**76.5**	**70**
12102312	13.4	77.9	40	**12102718**	**29.7**	**75.6**	**70**
12102318	14.0	77.6	45	**12102800**	**30.5**	**74.7**	**65**
12102400	14.7	77.3	55	**12102806**	**31.3**	**73.9**	**65**
12102406	15.6	77.1	60	**12102812**	**32.0**	**73.0**	**65**
12102412	**16.6**	**76.9**	**65**	**12102818**	**32.8**	**72.0**	**65**
12102418	**17.7**	**76.7**	**75**	**12102900**	**33.9**	**71.0**	**70**
12102419	**17.9**	**76.6**	**75**	**12102906**	**35.3**	**70.5**	**80**
12102500	**18.9**	**76.4**	**85**	**12102912**	**36.9**	**71.0**	**85**
12102505	**20.0**	**76.0**	**100**	**12102918**	**38.3**	**73.2**	**80**
12102506	**20.1**	**76.0**	**100**	**12102921**	**38.8**	**74.0**	**75**
12102509	**20.9**	**75.7**	**95**	**12102923**	**39.4**	**74.4**	**70**
12102512	**21.7**	**75.5**	**95**	**12103000**	**39.5**	**74.5**	**70**
12102518	**23.3**	**75.3**	**90**	12103006	39.9	76.2	55
12102600	**24.8**	**75.9**	**75**	12103012	40.1	77.8	50
12102606	**25.7**	**76.4**	**70**	12103018	40.4	78.9	40
12102612	**26.4**	**76.9**	**65**	12103100	40.7	79.8	35
12102618	**27.0**	**77.2**	**65**	12103106	41.1	80.3	35

Table S2. As in Table S1, except for Hurricane Lisa 14L 2010. The latitude of LMI for Hurricane Lisa is 20.4°N and it quickly weakened after reaching maximum intensity.

Date(yymmddhh)	Lat(°N)	Lon (°W)	Vmax(kts)	Date(yymmddhh)	Lat(°N)	Lon (°W)	Vmax(kts)
10092100	16.8	31.9	35	10092400	17.9	28.0	35
10092106	17.3	31.8	40	10092406	18.3	27.7	40
10092112	17.7	31.7	40	10092412	19.0	27.6	50
10092118	17.8	31.5	40	**10092418**	**19.7**	**27.7**	**60**
10092200	17.6	31.3	35	**10092421**	**20.0**	**27.7**	**65**
10092206	17.3	30.9	35	**10092500**	**20.4**	**27.8**	**75**
10092212	17.3	30.4	35	**10092506**	**21.3**	**28.0**	**70**
10092218	17.4	30.0	30	**10092512**	**22.3**	**28.3**	**60**
10092300	17.5	29.7	30	10092518	23.2	28.6	50
10092306	17.5	29.3	30	10092600	24.0	28.8	40
10092312	17.5	28.8	35	10092606	24.8	28.9	35
10092318	17.6	28.3	35				

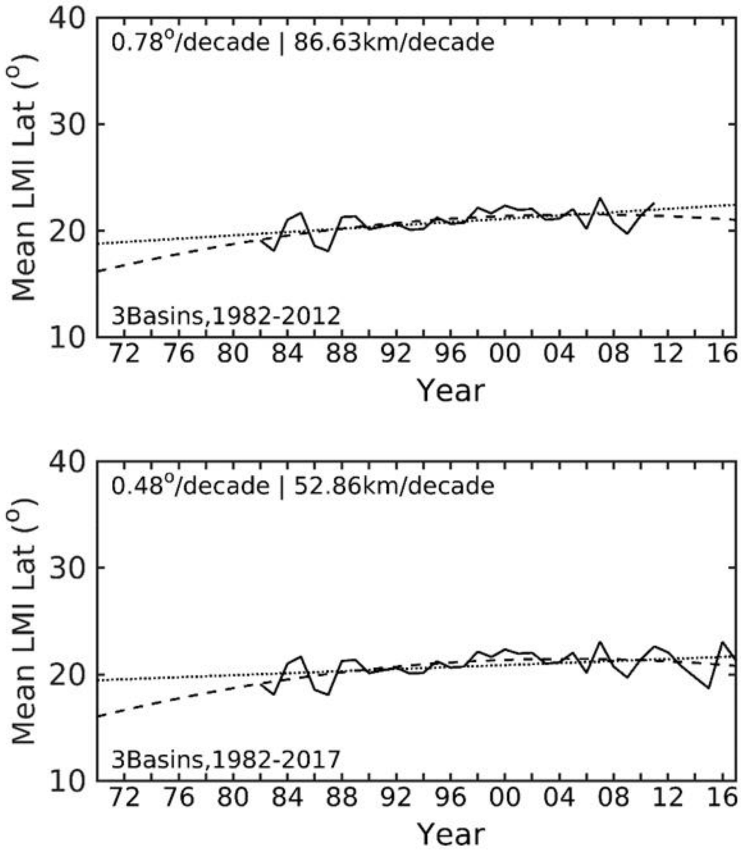

Fig. S1. The annual mean time series of the TC LMI latitudes and their trends for 1982-2012 (upper) and 1982-2017 (bottom) for 3 basins combined. Dotted and dashed lines respectively show the best fit linear and quadratic trends. The linear trends are respectively 0.78^{o} and 0.48^{o} per decade, which are statistically significant.

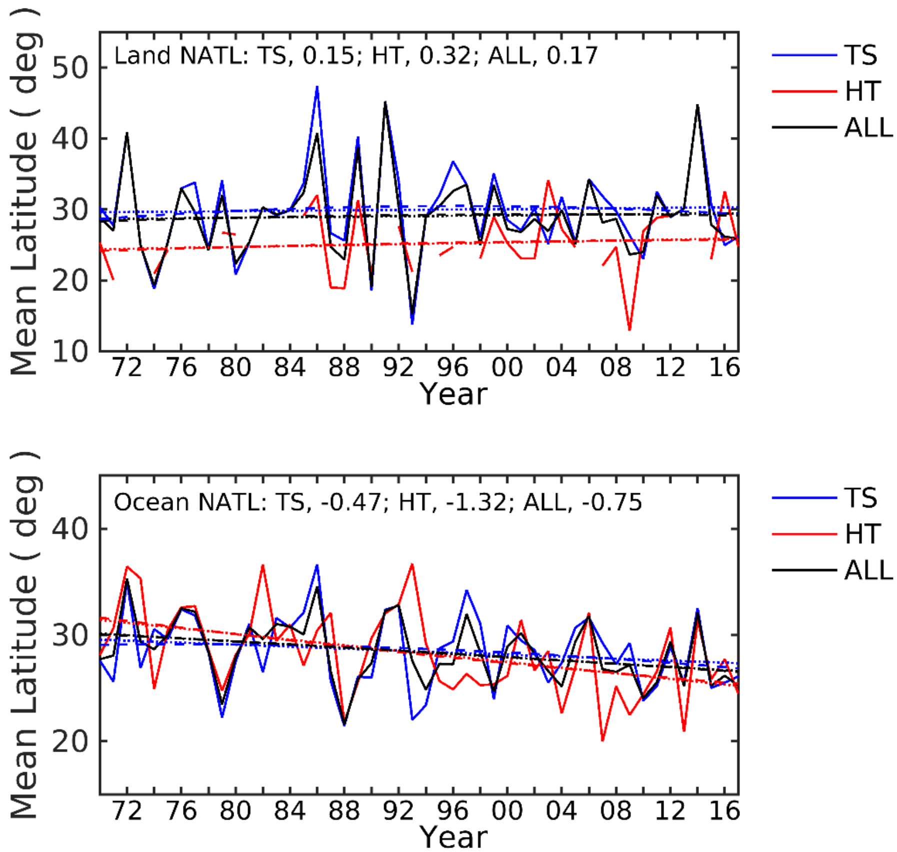

Fig. S2. 1970-2017 annual mean time series of TC latitudinal positions and their trends over land (upper) and ocean (bottom) for NATL. The blue, red, and dark solid curves are for TS, HT, and ALL storms, respectively. Dotted and dashed lines respectively show the best fit linear and quadratic trends. The linear trend values are shown in the top of each panel with unit degree per decade.

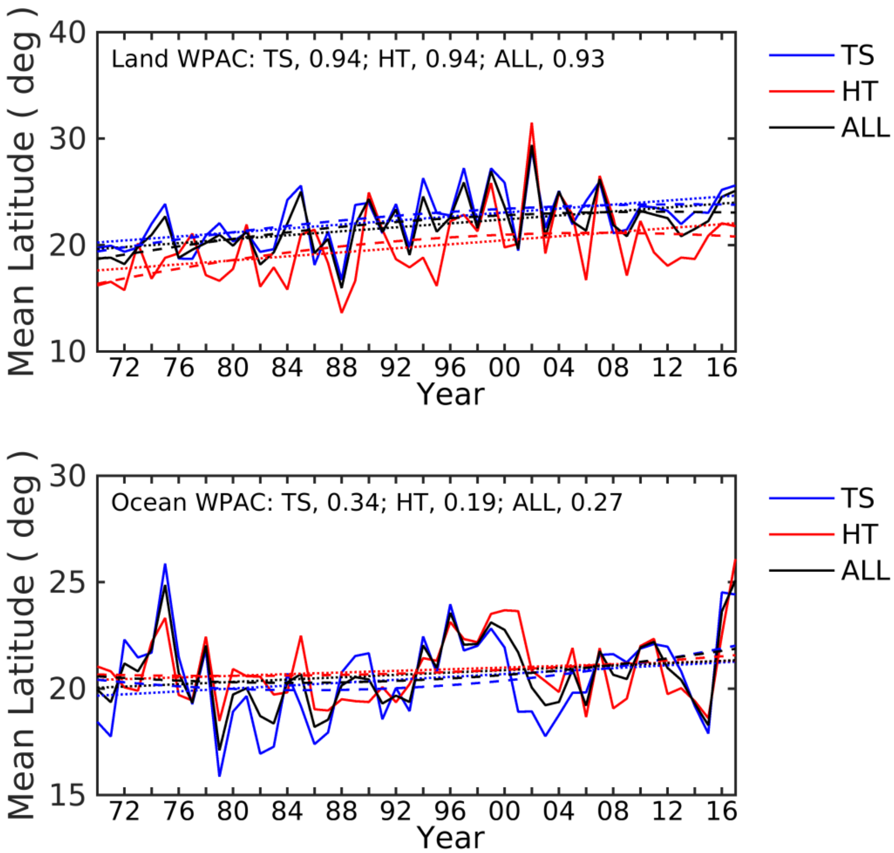

Fig. S3. As in Fig. S2 except for WPAC.

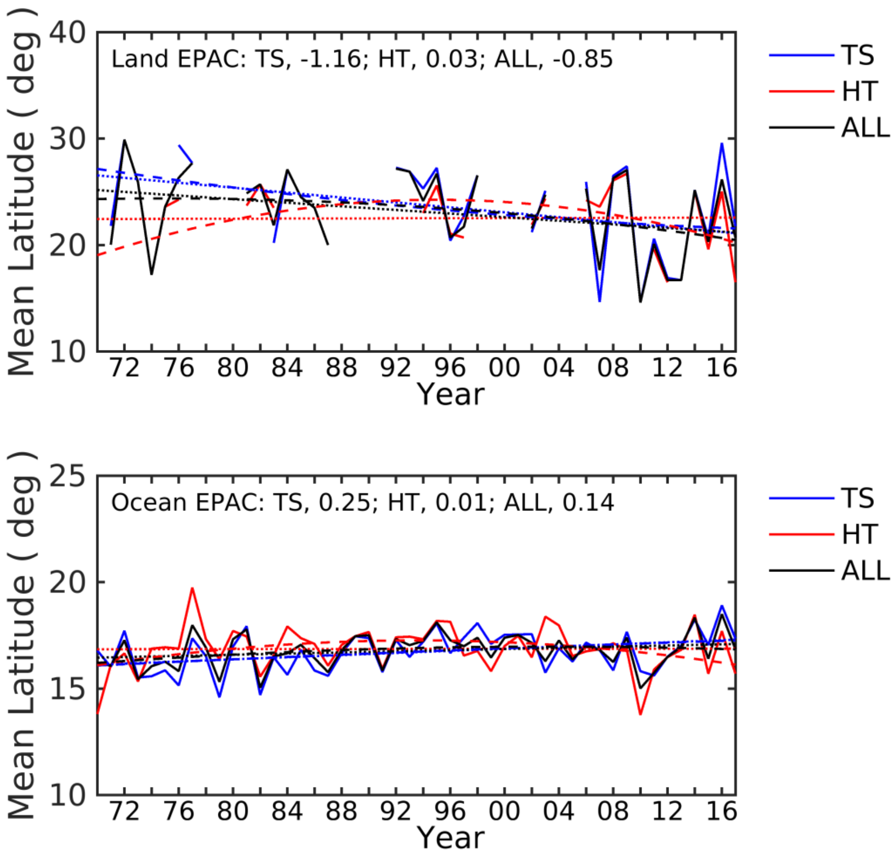

Fig. S4. As in Fig. S2 except for EPAC. Note that there are so few EPAC TCs making landfalls that the annual mean time series are not reliable for the trend analysis.

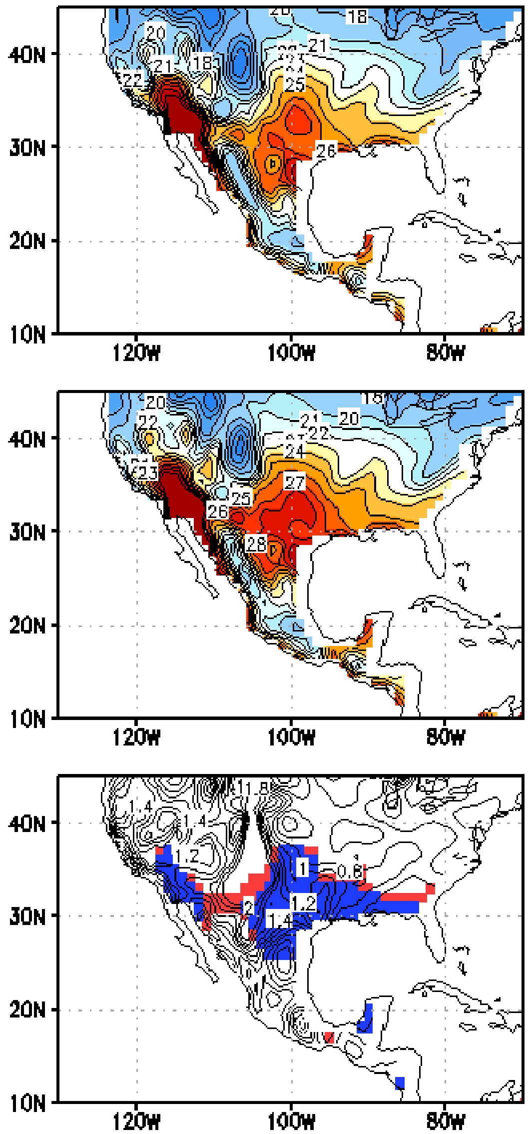

Fig. S5. 10year annual mean of ERAi SKT over North America during the Northern Hemisphere TC season for 1979-1988 (upper), 2007-2016 (middle), and the difference between 2007-2016 and 1979-1988 with blue indicating the area of averaged SKT greater than 24^{0}C for 1979-1988, and red for 2007-2016 (bottom).

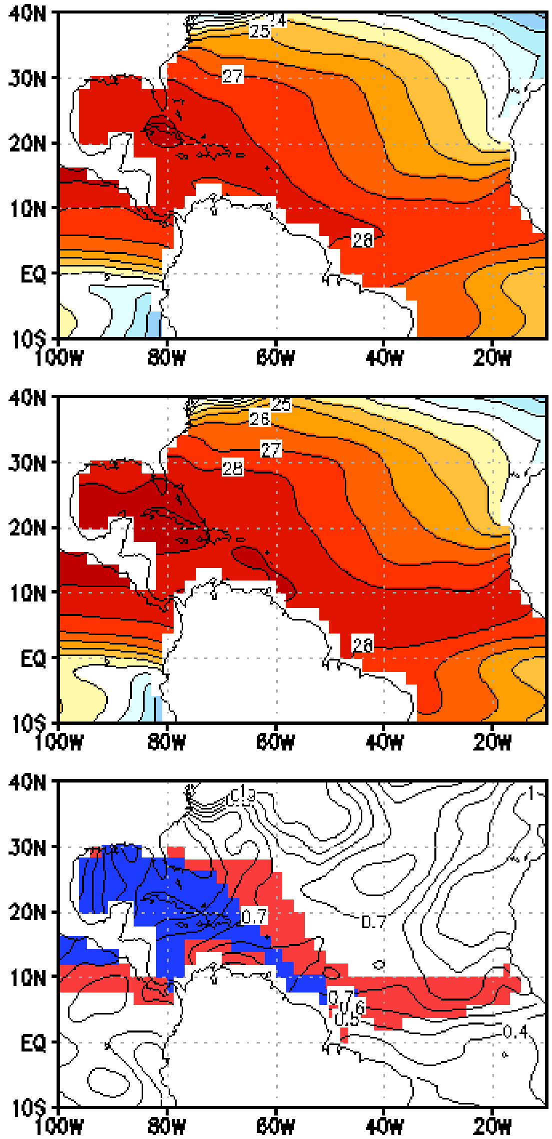

Fig. S6. 10 year annual mean of Pacific SST in Northern Hemisphere Hurricane/Typhoon season for 1970-1979 (upper), 2008-2017 (middle), and the difference between 2008-2017 and 1970-1979 with blue indicating the area of averaged SST greater than 28^{0}C for 1970-1979, and red for 2008-2017 (bottom).

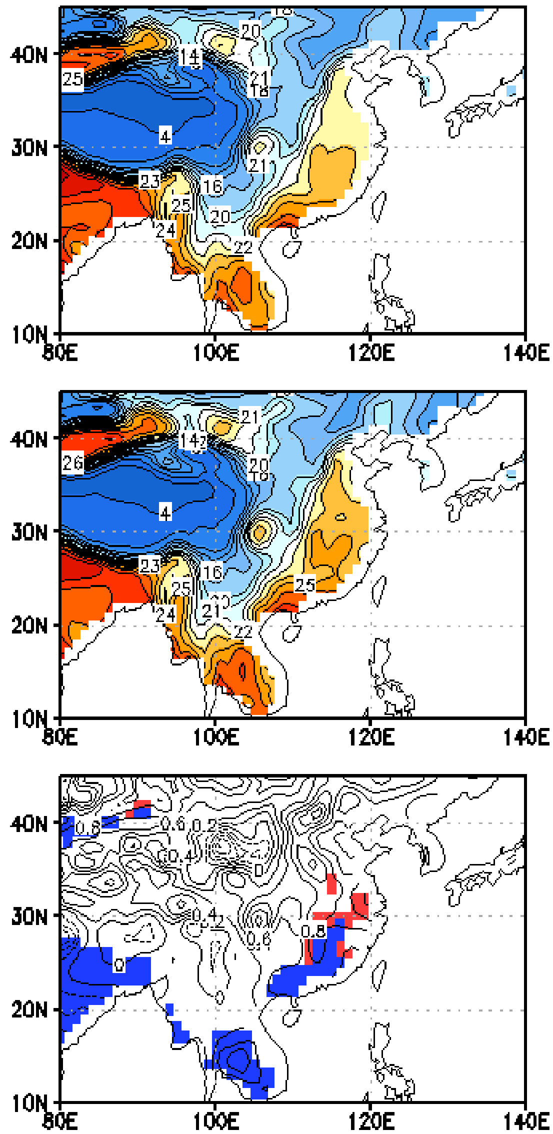

Fig. S7. 10 year annual mean of ERAi SKT in Northern Hemisphere Hurricane/Typhoon season for 1979-1988 (upper), 2007-2016 (middle), and the difference between 2007-2016 and 1979-1988 with blue indicating the area of averaged SKT greater than 24^0C for 1979-1988, and red for 2007-2016(bottom).

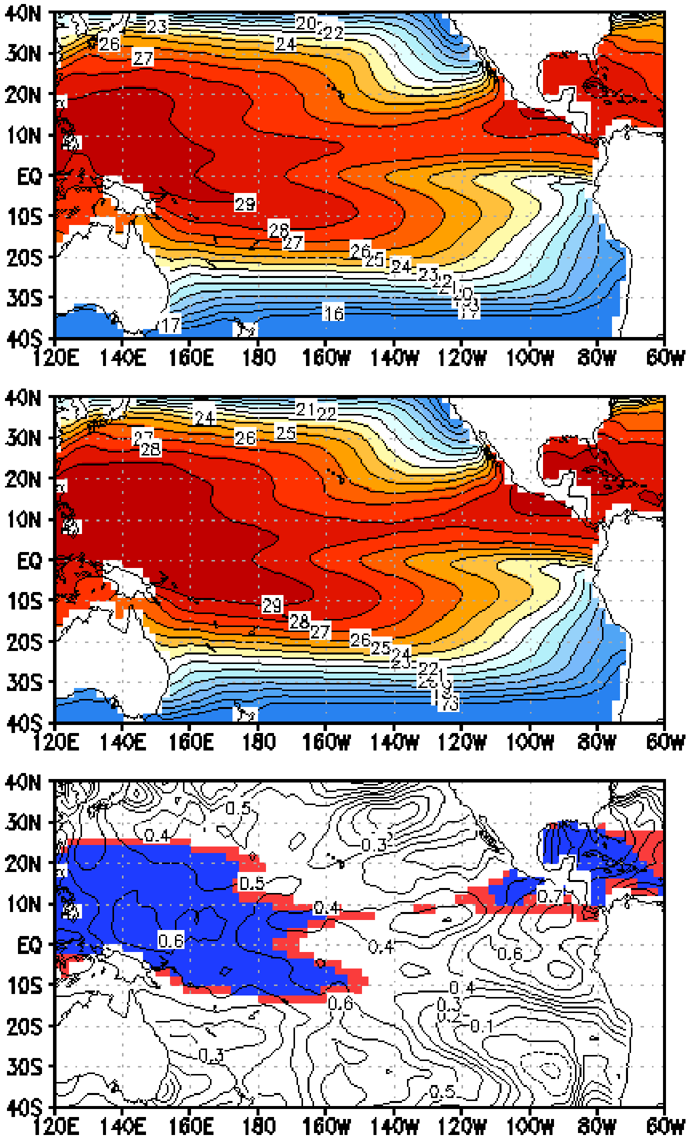

Fig. S8. 10 year annual mean of Pacific SST in Northern Hemisphere Hurricane/Typhoon season for 1970-1979 (upper), 2008-2017 (middle), and the difference between 2008-2017 and 1970-1979 with blue indicating the area of averaged SST greater than 28^{0}C for 1970-1979, and red for 2008-2017 (bottom).